Food and Chemical Toxicology 128 (2019) 68–80

Contents lists available at ScienceDirect

Food and Chemical Toxicology

journal homepage: www.elsevier.com/locate/foodchemtox

Distribution of methyl and isopropyl *N*-methylanthranilates and their metabolites in organs of rats treated with these two essential-oil constituents

Ana B. Miltojević[a,*], Nikola M. Stojanović[b], Pavle J. Randjelović[c], Niko S. Radulović[d,**]

[a] University of Niš, Faculty of Occupational Safety, Čarnojevića 10a, 18000, Niš, Serbia
[b] University of Niš, Faculty of Medicine, Zorana Đinđića 81, 18000, Niš, Serbia
[c] University of Niš, Faculty of Medicine, Institute of Physiology, Zorana Đinđića 81, 18000, Niš, Serbia
[d] University of Niš, Faculty of Sciences and Mathematics, Department of Chemistry, Višegradska 33, 18000, Niš, Serbia

ARTICLE INFO

Keywords:
Methyl *N*-Methylanthranilate
Isopropyl *N*-Methylanthranilate
Xenobiotic
Organs distribution
Metabolite identification
Multivariate statistical analysis

ABSTRACT

Two volatile alkaloids, methyl (MMA) and isopropyl *N*-methylanthranilates (IMA), identified in the essential oil of *Choisya ternata* Kunth (Rutaceae), have been proven to possess polypharmacological properties (anti-nociceptive, anti-inflammatory, gastro-, hepato-, nephroprotective activities, anxiolytic and antidepressant properties, and likewise an effect on diazepam-induced sleep). In the continuation of our investigation of their urinary-metabolite profiles, we performed GC-MS analyses of the diethyl-ether extracts of selected tissues (liver, kidneys, heart, brain, lungs, quadriceps femoris muscle, and spleen) of rats intraperitoneally treated with MMA or IMA (2 g kg^{-1}). Organ-metabolite profiles of MMA and IMA were qualitatively mutually analogous (varying only in the alcohol moiety of the metabolites), and generally analogous to their urinary-metabolite profiles. The greatest diversity and the highest overall amount of anthranilate metabolites was found in the hepatic tissue. The principal anthranilate-related compounds in the organs of rats treated with MMA, among 12 detected, were the products of ester hydrolysis, *N*-methylanthranilic and anthranilic acids. In the tissues of IMA-treated rats, among 16 compounds, the most abundant ones were the unmetabolized IMA and *N*-methylanthranilic acid. A collection of the compositional data regarding the anthranilate-related metabolites was statistically treated by multivariate statistical analysis that provided a better insight into the possible biotransformation pathways.

1. Introduction

Nowadays, a quarter of active principles that are used for medical purposes are isolated from plant material and more than ¾ are of plant origin (Miltojević et al., 2018). Plant-derived medicinal preparations have been used since ancient times (Tisserand and Young, 2014; Radulović et al., 2013c), while more widespread use of plant volatiles, specifically essential oils begun in the Middle Ages (Bakkali et al., 2008). The specific properties of essential oils, including their antioxidant, antibacterial, antifungal, antiviral, and various other pharmacological properties, were the inspiration for their usage in folk medicine, as well as the driving force of drug design and development. The review on biological effects of essential oils, including some toxicological assessment, was given by Bakkali and his co-workers (2008). Although biological activity of essential oils is often attributed to the activities of the major constituents or their synergism, we recently demonstrated that even minor secondary metabolites, frequently missed out during standard essential-oil analyses, may contribute significantly to the net biological activity of the oil or may even produce adverse effects (Radulović et al., 2011, 2013c).

Once inside an organism, pharmacologically active substances undergo different xenobiotic biotransformation pathways. The formed metabolites might either attain (Fura, 2006) or express the biological activity higher or lower than that of the parent compounds (Mitra et al., 2014) or they could even be toxic (Macherey and Dansette, 2008; Radulović et al., 2017). Many of the pharmacologically active metabolites are generated via cytochromes P450-catalyzed aromatic/aliphatic hydroxylation, or *O*- and *N*-dealkylation (Fura, 2006). Metabolite profiling, that includes identifying and quantifying xenobiotics and their metabolites within the organism, is one of the first and most important steps in their toxicological assessment, and drug design and development (Ufer et al., 2017). The obtained data may be crucial for the understanding of xenobiotic elimination routes, predicting drug-drug interactions, and anticipating xenobiotic safety concerns (Ufer

* Corresponding author.
** Corresponding author.
E-mail addresses: ana.miltojevic@znrfak.ni.ac.rs, anamiltojevic@yahoo.com (A.B. Miltojević), nikoradulovic@yahoo.com (N.S. Radulović).

https://doi.org/10.1016/j.fct.2019.03.039
Received 27 February 2019; Accepted 20 March 2019
Available online 23 March 2019
0278-6915/ © 2019 Elsevier Ltd. All rights reserved.

et al., 2017).

A study motivated by the ethnomedicinal use of Mexican orange, *Choisya ternata* Kunth (Rutaceae) (Radulović et al., 2011), resulted in the identification of two minor volatile alkaloids, methyl *N*-methylanthranilate (MMA) and isopropyl *N*-methylanthranilate (IMA), initially detected in its essential oil. It was the first time that IMA was identified in a sample of natural origin and it was named ternanthranin, while MMA was previously reported from a number of Rutaceae species. Subsequent studies dealt with the antioxidant (Radulović et al., 2015), antimicrobial (Miltojević et al., 2018) and various pharmacological activities of MMA and IMA. Both esters exhibited polypharmacological, panacea-like properties (Miltojević et al., 2018) including: antinociceptive (Gomes Pinheiro et al., 2014; Radulović et al., 2011), anti-inflammatory (Gomes Pinheiro et al., 2015), hepato- (Radulović et al., 2013d, 2017), nephro- (Radulović et al., 2015) and gastroprotective (Radulović et al., 2013a) activities, anxiolytic and antidepressant properties, as well as an effect on diazepam-induced sleep (Radulović et al., 2013b).

Moreover, MMA can be regarded as a constituent of the human everyday diet, since it is naturally present in various fruits and plants, or it is added artificially to confectionary products. Also, due to its pleasant olfactory properties, MMA is used in cosmetics and home cleaning products. A daily intake of MMA in Europe is estimated to be 1 μg kg^{-1} bodyweight (bw) day^{-1} for oral, and 2.7 μg kg^{-1} bw day^{-1} for cutaneous exposure (Radulović et al., 2011; SCCS, 2011). In a subchronic toxicity study of MMA in rats, at a dose of 2.25 g kg^{-1} bw, no mortality, no clinical signs of adverse effects and no abnormal gross autopsy findings in survivors were recorded (Gaunt, 1970). The acute oral LD_{50} of MMA was reported to be 3.7 g kg^{-1} bw for rats (SCCS, 2011). MMA and IMA at a dose of 100 mg kg^{-1} (*p.o.*) did not cause any alteration in motor function or spontaneous activity in treated mice, and at this dose, no signs of intoxication, such as convulsions, gastric ulcers or death, were noticed (Gomes Pinheiro et al., 2014). Additionally, the two anthranilate esters, applied on their own to rats, did not cause any significant kidney-tissue damage (200 mg kg^{-1}, *i.p.*, 7 days; Radulović et al., 2015), changes in liver morphology and function (200 mg kg^{-1}, *i.p.*, 7 days; Radulović et al., 2013d, 2017) and gastric lesions (200 mg kg^{-1}, *p.o.*; Radulović et al., 2013a). On the other hand, a 1.0% solution of MMA was considered to be phototoxic as it produced reactions in 40% of treated human subjects (SCCS, 2011).

Prompted by the abovementioned results and the possible pharmacological application of IMA and MMA, as well as due to constant exposure to MMA via oral and skin routes, we evaluated the metabolism of these two xenobiotic compounds in rats. In continuation of our recent investigation of their urinary-metabolite profiles (Radulović et al., 2017), we decided to investigate the distribution of methyl and isopropyl *N*-methylanthranilates and their metabolites in selected organs of rats acutely treated with these two essential-oil constituents (2 g kg^{-1}, *i.p.*). In our previous study, we found that both anthranilates underwent the same biotransformation pathways. However, in the case of IMA urinary-metabolic profile, among 16 anthranilic acid-related compounds, products of aromatic core hydroxylation, more specifically isopropyl 5-hydroxy-*N*-methylanthranilate, isopropyl 5-hydroxyanthranilate, and isopropyl 3-hydroxyanthranilate, were the major metabolites. 2-(Methylamino)benzamide and *N*-methylanthranilic acid, the products of ester group transformation, were the principal metabolites of MMA, among 14 other detected biotransformation products. Herein, we evaluated the amounts of the mentioned xenobiotics and their metabolites in the liver, kidneys, heart, lungs, brain, quadriceps femoris muscle, and spleen of rats treated with these two substances. We wished to upgrade the descriptive approach that was presented in our previous publication relating to the mutual connections among the parent compounds and metabolites (Radulović et al., 2017), and in this paper, the quantitative metabolite profiles of MMA and IMA in different organs that were obtained through the application of GC-MS were subjected to multivariate statistical analyses (MVA). Such an approach enabled us to analyze and functionally interpret the complex interactions between the detected metabolites and the parent compounds.

2. Materials and methods

2.1. General

Methyl and isopropyl esters of *N*-methylanthranilic acid were synthesized as described previously (Radulović et al., 2011). Ketamine (Ketamidor 10%) was purchased from Richter Pharma AG (Wels, Austria). All other reagents and solvents were obtained from commercial sources (Sigma-Aldrich, St. Louis, Missouri, USA; Merck, Darmstadt, Germany; Carl Roth, Karlsruhe, Germany) and used as received, except that the solvents were purified by distillation.

2.2. GC-MS analyses

Gas chromatography-mass spectrometry (GC-MS) analyses were repeated three times for each sample using an HP 6890N gas chromatograph coupled with an HP 5975B mass-selective detector (Hewlett-Packard, Palo Alto, California, USA). The gas chromatograph was equipped with a DB-5MS fused silica capillary column (5% phenyl methyl siloxane, 30 m × 0.25 mm, film thickness 0.25 μm; Agilent Technologies, Palo Alto, California, USA). The oven temperature was raised linearly from 70 to 315 °C at a heating rate of 5 °C min^{-1} and then held isothermally for 10 min. Helium at a flow rate of 1 ml min^{-1} was used as the carrier gas. The injector and interface were maintained at 250 and 320 °C, respectively. The samples, 1 μl of the solutions of tissue homogenate extracts and standard solutions of MMA and IMA in ethyl acetate, were injected in a pulsed split mode (the flow rate was 1.5 ml min^{-1} for the first 0.5 min and then set to 1 ml min^{-1} for the remainder of the analysis; split ratio 40:1). The mass-selective detector was operated at the ionization energy of 70 eV in the *m/z* 35–500 range with a scanning speed of 0.34 s. The selected ion monitoring (SIM) mode was used for quantitation. The selector and quantifier ions are given in the corresponding tables in the Results and discussion section.

Initially, the percentage composition was computed from GC-peak areas without the use of correction factors. The linear retention indices relative to the retention times of C_9–C_{19} *n*-alkanes on the DB-5MS column were calculated according to Van Den Dool and Kratz (1963). Qualitative analyses of the mentioned samples were firstly based on the comparison of their mass spectra with those of authentic standards, as well as those from Wiley 11 and NIST2017, the analysis of the fragmentation patterns from their mass spectra, and finally, wherever possible, identification was achieved by GC co-injection with an authentic sample.

For the purpose of quantitation of MMA, IMA, as well as their metabolites, in the rat tissue homogenates, a series of standard solutions of MMA and IMA in ethyl acetate, were prepared, using anthracene and naphthalene as internal standards, respectively. The concentrations of the standard solutions were 0.5, 0.1, 0.05, 0.01, and 0.005 mg ml^{-1}, and were prepared by diluting the stock solution of MMA and IMA (1 mg ml^{-1}) in ethyl acetate. The concentration of the internal standards was equal to the concentrations of MMA and IMA. The calibration curves–areas under the curve versus the concentration of MMA, IMA, as well as the internal standards–were constructed. Standard and calibration solutions were stored at 4 °C prior to analysis.

2.3. Animals

Healthy adult male and female Wistar rats weighing 200–250 g, obtained from the Vivarium of the Scientific Research Center for Biomedicine, Faculty of Medicine, University of Niš, were maintained under standard laboratory conditions: 22 ± 2 °C, 60% humidity and 12/12 (light/dark) cycle, with food and water available *ad libitum*. All experiments were performed in compliance with the legislation

covering the use of animals for scientific purposes (EU Directive, 2010/63/EU for animal experiments) and approved by the local Ethics committee (number 01-7289-11).

2.4. Experimental design

The animals fasted 24 h before the commencement of the experiment and were randomly divided into three groups, two experimental and one control, consisting of 6 animals each. MMA or IMA dissolved in olive oil were intraperitoneally (*i.p.*) given to the animals of the experimental groups at a dose of 2 g kg^{-1}. The control group received only olive oil (2 ml kg^{-1}). One hour following the application, the animals were sacrificed by an overdose of ketamine. The organs were removed, washed with ice-cold physiological saline, dried, frozen and kept at −80 °C until analyses. The following organs were chosen for the study: liver, kidneys, heart, brain, lungs, quadriceps femoris muscle, and spleen.

A part of the tissue, in the case of the liver, or the whole tissue was weighed on a balance, placed in a mortar, and cut into smaller pieces with a scalpel. A saturated solution of NaCl (3 ml) and *ca.* 5 g of quartz sand were added and the mixture was homogenized with a pestle. The magnetically stirred homogenate was subjected to exhaustive continuous extraction with diethyl ether. The organic layer was filtered through NaCl and additionally dried over anhydrous $MgSO_4$. The solvent was evaporated under a stream of dry nitrogen. To each sample, 1 ml of the internal standard solution (anthracene, in the case of MMA, or naphthalene, in the case of IMA, dissolved in ethyl acetate) was added, and the resulting solution was checked for turbidity and complete dissolution. The sample was transferred into a GC vial and subsequently analyzed by GC-MS.

2.5. Method validation

GC-MS methods for the detection and/or quantitation of MMA, IMA and their metabolites in rat tissues were developed and validated under the GC-MS operating conditions described above. Blank rat tissue samples collected from adult male and female Wistar rats were used for calibration and validation purposes, while the internal standard method was used for quantitation purposes. The calibration curves were based on linear regression analysis using the ratio of the analyte peak area related to the internal standard.

GC-MS method validation parameters were as follows: tissue samples including calibrators and quality controls were tested for selectivity and no interferences were found. The linearity was established to be within 0.005–0.5 mg ml^{-1} with regression coefficients greater than 0.999 for MMA and IMA. For both anthranilates, the detection limit (LOD, S/N > 3) was 0.25 μg ml^{-1}, while the lower limits of quantitation (LLOQ, S/N > 8) were 2.5 μg ml^{-1}, respectively.

2.6. Computational methods

Geometry optimizations (MM2 molecular mechanics force field method) and calculation of molecular properties, especially those associated with blood-brain barrier (BBB) permeability, of MMA, IMA and their metabolites were performed using Chem3D Ultra 16.0 software package (CambridgeSoft). The following were calculated: clogP, number of H-bond acceptors and donors, polar surface area, ovality, number of rotatable bonds, pKa.

2.7. Statistical analysis

Results were expressed as the mean ± SD. Statistically significant differences were determined by one-way analysis of variance (ANOVA) followed by Tukey's post hoc test for multiple comparisons (GraphPad Prism version 5.03, San Diego, CA, USA). Probability values (p) less than 0.05 were considered to be statistically significant.

Principal component analysis (PCA) and agglomerative hierarchical cluster analysis (AHC) were performed using the Excel program plug-in XLSTAT version 2018.7.55098. Both methods were applied utilizing the content of the extract constituents in mg per gram of the analyzed tissue as original variables (only constituents that were present in the organs in the amounts higher than 0.009 and 0.01 mg g^{-1} in the case of rats treated with MMA and IMA, respectively, were taken into account). The AHC was determined using Pearson dissimilarity (aggregation criterion: simple linkage, unweighted pair-group average, and complete linkage) and Euclidean distances (aggregation criterion: weighted pair-group average, unweighted pair-group average, and Ward's method). Group definition was based on Pearson correlation, using complete linkage and unweighted pair-group average method.

3. Results and discussion

Gas chromatography-mass spectrometry toxicological methods were developed and validated, and applied for the detection and/or quantitation of MMA or IMA and their metabolites in selected organs of rats intraperitoneally treated with these substances, at a dose of 2 g kg^{-1}. Our experiments were commenced by the validation of the GC-MS method. The recovery, limit of detection and limit of linearity studies were performed. The recovery rates using tissue homogenates as the matrices were 85.0 and 91.2% for MMA and IMA, respectively, at the concentration of 1 μg ml^{-1} for each analyte. The calibration curves using SIM-peak areas for IMA and MMA were linear over the concentration range of 0.005–0.5 mg ml^{-1} with correlation coefficients greater than 0.999. The detection limits of MMA and IMA by GC-MS were 0.25 μg ml^{-1}.

The dose of the two anthranilates that was intraperitoneally administered to rats, 2 g kg^{-1}, was significantly higher than their pharmacologically active doses (Radulović et al., 2011, 2013a, 2013b, 2013d, 2015; Gomes Pinheiro et al., 2014, 2015). This mode of application and such a high dose were chosen to provide a sufficient amount of the metabolites for GC-MS analyses. Even at such a high dose, no adverse effects (*i.e.* no evident signs of toxicity: no abnormal gross autopsy findings and no mortality) were noted for the treated rats, that is in agreement with the previous study for MMA (Gaunt, 1970). One hour after the application, the animals were sacrificed and the contents of the xenobiotics in selected organs (liver, kidneys, heart, brain, lungs, quadriceps femoris muscle, and spleen) were analyzed by GC-MS. The identified constituents (only the ones related to anthranilic acid) in the diethyl-ether extracts of the homogenates of the chosen tissues, RI values and methods of identification are combined in Tables 1 and 2. Prior to single ion monitoring (SIM) that was used for quantitation purposes, full scan GC-MS runs were performed that were utilized for the identification of MMA and IMA metabolites. The identification was based on the comparison of their linear retention indices and MSes with the data acquired in our previous research on MMA and IMA urinary-metabolite profiles (Radulović et al., 2017). During this previous study, we also prepared pure synthetic or isolated substances that were used herein as standards either for identification or quantitation (Radulović et al., 2017). The total ion current chromatograms (TIC) of the liver homogenate extracts containing IMA and its major metabolites is depicted in Fig. 1. The amounts of the anthranilic acid-related constituent identified in the diethyl-ether extracts of the homogenates of the chosen tissues per gram of the respective organ are given in Tables 3 and 4.

Organ-metabolite profiles of MMA and IMA were qualitatively mutually analogous (varying only in the alcohol moiety of the metabolites), and generally analogous to the urinary-metabolite profiles (Radulović et al., 2017). In total, 12 and 16 anthranilate-related compounds were found in the analyzed tissues of rats treated with MMA and IMA, respectively. The greatest diversity of the metabolites was found in the liver, the major organ in the detoxification process. The detected compounds in the liver tissue were the unmetabolized MMA/IMA, the product of their hydrolysis - *N*-methylanthranilic acid

Table 1
GC-MS metabolite profile of the diethyl-ether extracts of the homogenates of the chosen tissues of MMA-treated rats.

N°[a]	RI	IdenMeth[b]	Selector and quantifier ions[c]	Structure	Abbreviation	Name
1	995	RI, MS, CoI	65, 66, <u>93</u>	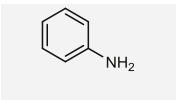	An	Aniline
2	1081	RI, MS, CoI	77, <u>106</u>, 107	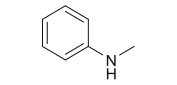	MAn	*N*-Methylaniline
3	1169	RI, MS, CoI	77, <u>105</u>, 122	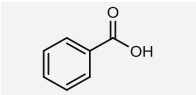	BA	Benzoic acid
4	1350	RI, MS, CoI	92, <u>119</u>, 151	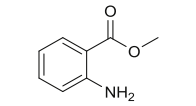	MA	Methyl anthranilate
5	1415	RI, MS, CoI	105, 132, <u>165</u>	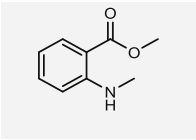	MMA	Methyl *N*-methylanthranilate
6	1423	RI, MS, CoI	92, <u>119</u>, 137	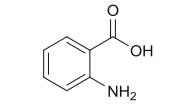	AA	Anthranilic acid
7	1466	RI, MS	104, 133, <u>151</u>	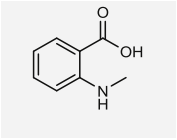	NMAA	*N*-Methylanthranilic acid
8	1571	RI, MS	133, <u>151</u>, 179	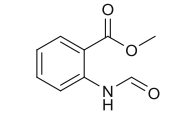	MFA	Methyl *N*-formylanthranilate
9	1632	RI, MS, CoI	<u>107</u>, 135, 167	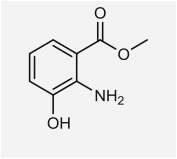	3-HMA	Methyl 3-hydroxyanthranilate
10	1664	RI, MS, CoI	107, <u>135</u>, 167	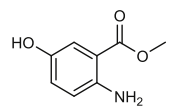	5-HMA	Methyl 5-hydroxyanthranilate
11	1722	RI, MS, CoI	120, 148, <u>181</u>	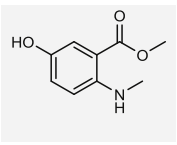	5-HMMA	Methyl 5-hydroxy-*N*-methylanthranilate
12	1811	RI, MS, CoI	120, 148, <u>181</u>	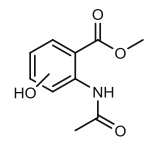	HMAcA	Methyl 3(or 5)-hydroxy-*N*-acetylanthranilate

[a] Compounds listed in order of elution on DB-5MS column (RI: experimentally determined retention indices on the mentioned column by co-injection of a homologous series of *n*-alkanes C_9–C_{19}).

[b] RI, constituent identified by retention index matching; MS, constituent identified by mass spectra comparison; CoI, constituent identity confirmed by GC co-injection of the authentic sample.

[c] Quantifier ions are underlined.

Table 2
GC-MS metabolite profile of the diethyl-ether extracts of the homogenates of the chosen tissues of IMA-treated rats.

N°[a]	RI	IdenMeth[b]	Selector and quantifier ions[c]	Structure	Abbreviation	Name
1	995	RI, MS, CoI	65, 66, <u>93</u>	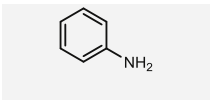	An	Aniline
2	1081	RI, MS, CoI	77, <u>106</u>, 107	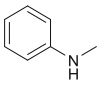	MAn	*N*-Methylaniline
3	1169	RI, MS, CoI	77, <u>105</u>, 122	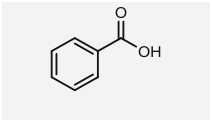	BA	Benzoic acid
4	1423	RI, MS, CoI	92, <u>119</u>, 137	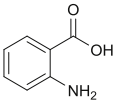	AA	Anthranilic acid
5	1452	RI, MS, CoI	<u>119</u>, 137, 179	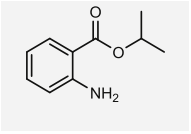	IA	Isopropyl anthranilate
6	1466	RI, MS	104, 133, <u>151</u>	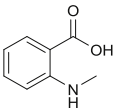	NMAA	*N*-Methylanthranilic acid
7	1517	RI, MS, CoI	<u>105</u>, 151, 193	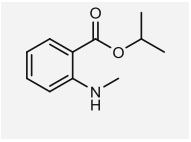	IMA	Isopropyl *N*-methylanthranilate
8	1528	RI, MS	<u>121</u>, 138, 180	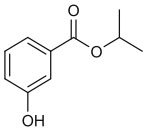	3-HIB	Isopropyl 3-hydroxybenzoate
9	1536	RI, MS	<u>121</u>, 167, 209	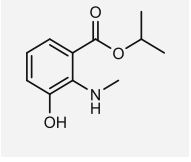	3-HIMA	Isopropyl 3-hydroxy-*N*-methylanthranilate
10	1604	RI, MS, CoI	104, 133, <u>150</u>	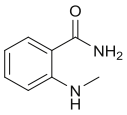	3-MABA	2-(Methylamino)benzamide
11	1671	RI, MS	<u>119</u>, 137, 179	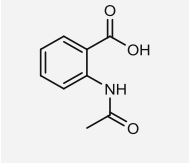	AcAA	*N*-Acetylanthranilic acid
12	1677	RI, MS	<u>119</u>, 137, 221	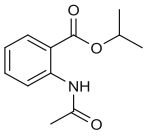	IAcA	Isopropyl *N*-acetylanthranilate
13	1726	RI, MS, CoI	107, <u>135</u>, 195	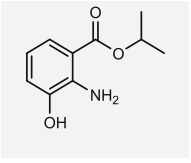	3-HIA	Isopropyl 3-hydroxyanthranilate

(*continued on next page*)

Table 2 (*continued*)

N°[a]	RI	IdenMeth[b]	Selector and quantifier ions[c]	Structure	Abbreviation	Name
14	1760	RI, MS, CoI	135, 153, 195	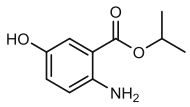	5-HIA	Isopropyl 5-hydroxyanthranilate
15	1815	RI, MS, CoI	121, 167, 209	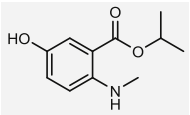	5-HIMA	Isopropyl 5-hydroxy-*N*-methylanthranilate
16	1822	RI, MS, CoI	135, 177, 195	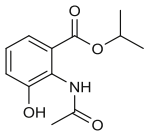	3-HIAcA	Isopropyl 3-hydroxy-*N*-acetylanthranilate

[a] Compounds listed in order of elution on DB-5MS column (RI: experimentally determined retention indices on the mentioned column by co-injection of a homologous series of *n*-alkanes C_9–C_{19}).

[b] RI, constituent identified by retention index matching; MS, constituent identified by mass spectra comparison; CoI, constituent identity confirmed by GC co-injection of the authentic sample.

[c] Quantifier ions are underlined.

(NMAA), *N*-demethylation products - methyl (MA)/isopropyl anthranilates (IA), as well as the product of their subsequent hydrolysis and *N*-demethylation - anthranilic acid (AA). The products of hydroxylation of the aromatic core, methyl and isopropyl esters of 3- and 5-hydroxyanthranilic acids and 5-hydroxy-*N*-methylanthranilic acid, were found in the liver, only in traces (i.e. between LOD and LLOQ), while in the case of IMA isopropyl 3-hydroxy-*N*-methylanthranilate (3-HIMA) and isopropyl 3-hydroxybenzoate (3-HIB) were detected, as well. Also, the liver of MMA/IMA-treated rats contained traces of aniline (An), *N*-methylaniline (MAn) and benzoic acid (BA), while 2-(methylamino) benzamide (2-MABA) was detected in the liver of IMA-treated rats. For MMA, among the detected anthranilate-related compound, the liver contained the highest amount of AA, followed by NMAA, and MMA. In the homogenates of the livers of female rats treated with IMA, the unmetabolized substance was the most abundant compound present, followed by NMAA, whereas the male rat liver contained a quantifiable amount of NMAA and only traces of all other detected anthranilate-related compounds.

The hepatic metabolism of MMA and IMA is in general agreement with that of anthranilic acid esters. It is known that in rodents (and humans) methyl *N*-methylanthranilate undergoes hydrolysis, principally in the liver, that is followed by *N*-demethylation, to yield anthranilic acid. Anthranilic acid could also be formed by an inversed order of metabolic steps (first *N*-demethylation, then hydrolysis), or both orders of events could operate simultaneously, as well (Radulović et al., 2017; Yamaori et al., 2005). All of the detected metabolites, as well as the parent compounds, are excreted via urine (SCCS, 2011 and references cited therein), which was confirmed in our previous study (Radulović et al., 2017). Hydrolysis of anthranilic acid esters is most likely catalyzed by carboxylesterases, located in various tissues, being most abundant in hepatocytes (Heymann, 1980). The process of *N*-demethylation is known to be catalyzed by cytochrome P450 (Yamaori et al., 2005) that initially hydroxylates the *N*-methyl group to form an aminal, which subsequently decomposes to give *N*-demethylated products (Radulović et al., 2017).

The principal difference between the organ- and urinary-metabolite (Radulović et al., 2017) profiles was in the relative abundances of 2-(methylamino)benzamide and the hydroxylated metabolites. Although 2-(methylamino)benzamide was the principal metabolite found in the urine of rats treated with MMA, comprising ca. 37% of the total extracted GC-MS-analyzable anthranilate-related compounds, and it comprised ca. 7% of the extract of the urine of rats treated with IMA, it was not found in the homogenates of the analyzed organs of MMA-treated animals and was a minor constituent (trace amounts) of IMA-

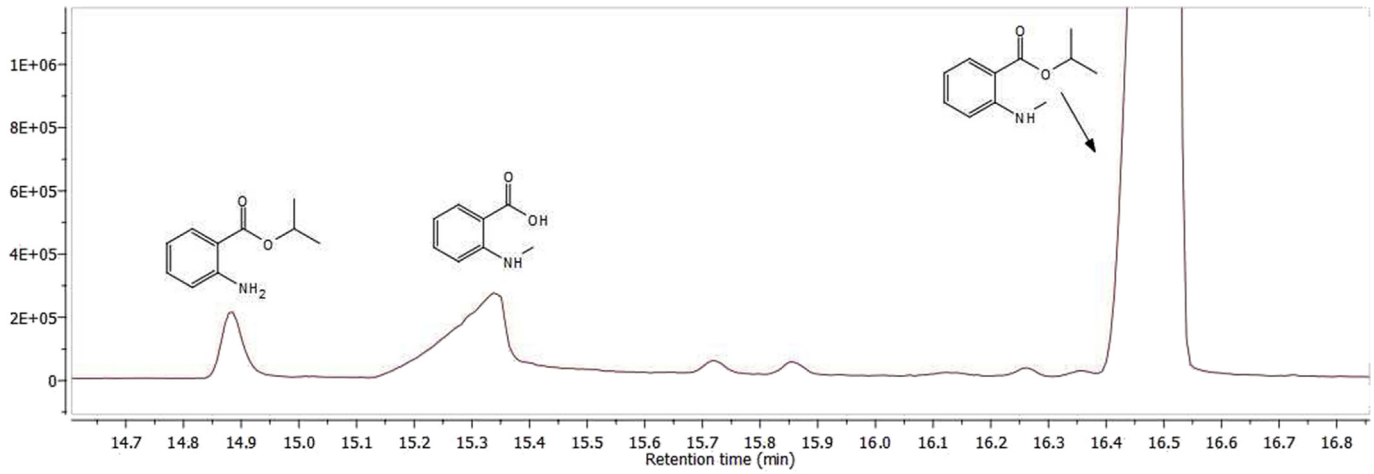

Fig. 1. The expansion of the total ion current chromatograms (TIC) of the liver homogenate extract containing ternanthranin and its principal metabolites.

Table 3
The distribution of MMA and its metabolites in the diethyl-ether extracts of the homogenates of the chosen tissues of rats treated with MMA (2 g kg^{-1} b.w., *i.p.*) expressed in milligrams of anthranilate-related metabolite per gram of organ tissue.

Compound	Gender	Liver	Kidneys	Heart	Brain	Lungs	Muscles	Spleen	Total[a]
MMA	f	0.020 ± 0.007	0.103 ± 0.007	0.045 ± 0.001	0.066 ± 0.004	0.023 ± 0.009	tr	tr	0.257
	m	0.011 ± 0.008	0.064 ± 0.002	0.021 ± 0.005	0.065 ± 0.002	tr	0.057 ± 0.009	0.050 ± 0.005	0.268
NMAA	f	0.855 ± 0.006	0.161 ± 0.009	0.298 ± 0.007	0.039 ± 0.007	0.027 ± 0.009	0.063 ± 0.004	tr	1.577
	m	0.749 ± 0.007	0.076 ± 0.002	0.259 ± 0.002	0.045 ± 0.007	0.015 ± 0.007	tr	tr	1.250
MA	f	tr	tr	tr	tr	-	tr	tr	tr
	m	tr	tr	tr	0.012 ± 0.006	-	tr	tr	0.013
AA	f	1.18 ± 0.04	tr	0.037 ± 0.008	tr	tr	-	-	1.466
	m	0.703 ± 0.005	tr	tr	tr	tr	-	-	0.847
3-HMA	f	tr	-	-	-	-	-	-	tr
	m	tr	-	-	-	-	-	-	tr
5-HMA	f	tr	-	-	-	-	-	-	tr
	m	tr	-	-	-	-	-	-	tr
5-HMMA	f	tr	tr	tr	tr	tr	tr	-	tr
	m	tr	tr	tr	tr	tr	tr	-	tr
An	f	tr	tr	-	-	-	-	-	tr
	m	tr	tr	-	-	-	-	-	tr
MAn	f	tr	tr	tr	tr	tr	-	tr	tr
	m	tr	tr	tr	tr	tr	-	tr	tr
BA	f	tr	-	-	-	-	-	-	tr
	m	tr	-	-	-	-	-	-	tr
HMAcA	f	tr	-	-	-	-	-	-	tr
	m	tr	-	-	-	-	-	-	tr
MFA	f	tr	-	-	-	-	-	-	tr
	m	tr	-	-	-	-	-	-	tr
Total female rats[a]		2.375	0.279	0.415	0.109	0.053	0.069	tr	3.300
Total male rats[a]		1.676	0.147	0.304	0.127	0.016	0.057	0.050	2.377

[a] Recalculated to the mass of MMA, - Compound not detected, tr – trace, i.e. between LOD and LLOQ for MMA.

Table 4
The distribution of IMA and its metabolites in the diethyl-ether extracts of the homogenates of the chosen tissues of rats treated with IMA (2 g kg^{-1} b.w., *i.p.*) expressed in milligrams of anthranilate-related metabolite per gram of organ tissue.

Compound	Gender	Liver	Kidneys	Heart	Brain	Lungs	Muscles	Spleen	Total[a]
IMA	f	0.105 ± 0.006	0.086 ± 0.006	0.074 ± 0.004	0.159 ± 0.008	0.058 ± 0.004	-	tr	0.482
	m	tr	0.078 ± 0.004	tr	0.031 ± 0.003	tr	-	tr	0.109
NMAA	f	0.080 ± 0.009	tr	tr	-	0.047 ± 0.008	-	tr	0.162
	m	0.020 ± 0.002	tr	tr	-	tr	-	tr	0.026
IA	f	tr	tr	tr	0.037 ± 0.004	tr	-	tr	0.040
	m	tr	tr	tr	tr	tr	-	tr	tr
AA	f	tr	tr	-	-	tr	-	-	tr
	m	tr	tr	-	-	tr	-	-	tr
3-HIA	f	tr	-	-	-	-	-	-	tr
	m	tr	-	-	-	-	-	-	tr
3-HIMA	f	tr	-	-	-	-	-	-	tr
	m	tr	-	-	-	-	-	-	tr
5-HIA	f	tr	-	-	-	-	-	-	tr
	m	tr	-	-	-	-	-	-	tr
5-HIMA	f	tr	tr	-	-	-	-	-	tr
	m	tr	tr	-	-	-	-	-	tr
An	f	tr	-	-	-	-	-	-	tr
	m	tr	-	-	-	-	-	-	tr
MAn	f	tr	tr	tr	-	tr	-	tr	tr
	m	tr	tr	tr	-	tr	-	tr	tr
BA	f	tr	tr	tr	tr	tr	-	tr	tr
	m	tr	tr	tr	tr	tr	-	tr	tr
3-HIB	f	tr	tr	-	-	tr	-	tr	tr
	m	tr	tr	-	-	tr	-	tr	tr
3-MABA	f	tr	-	-	-	-	-	-	tr
	m	tr	-	-	-	-	-	-	tr
AcAA	f	tr	tr	tr	-	-	-	tr	tr
	m	tr	tr	tr	-	-	-	tr	tr
IAcA	f	tr	tr	tr	-	tr	-	tr	tr
	m	tr	tr	tr	-	tr	-	tr	tr
3-HIAcA	f	tr	tr	-	-	-	-	-	tr
	m	tr	tr	-	-	-	-	-	tr
Total female rats[a]		0.207	0.086	0.074	0.199	0.118	-	tr	0.684
Total male rats[a]		0.026	0.078	tr	0.031	tr	-	tr	0.135

[a] Recalculated to the mass of IMA, - Compound not detected, tr – trace, i.e. between LOD and LLOQ for IMA.

treated animal livers. Moreover, neither of the organ-metabolite profiles displayed 2-aminobenzamide (anthranilamide), that comprised ca. 2% of the extract of the urine of MMA-treated rats and was found in traces in the urine of IMA-treated rats. This was in agreement with the findings of Naito et al. (1984) that found 2-aminobenzamide in the bile, but could not detect it in the anthranilic acid-treated isolated perfused livers of rats. These authors supposed that the amide is non-enzymatically produced in the bile from anthraniloyl glucuronide. Although bile metabolites are feces-eliminated, we found the mentioned amides as urine metabolites (Radulović et al., 2017). Thus, it seems that the amides accumulate specifically in the bile, but their formation should probably be traced to the liver.

Another difference between the organ- and urine-metabolite profiles was the abundance of the hydroxylated metabolites that were the major ones in the case of the urine of rats treated with IMA, comprising ca. 60% of the total extracted GC-MS-analyzable compounds, while in the case of MMA they comprised around 13% (Radulović et al., 2017). On the other hand, isopropyl and methyl esters of 3-hydroxy- and 5-hydroxyanthranilic acids were present only in the liver (in traces). Also, isopropyl ester of 3-hydroxy-*N*-methylanthranilic acid was detected in the liver of IMA-treated rats, while the liver of MMA-treated animals did not contain the corresponding metabolite. Isopropyl 5-hydroxy-*N*-methylanthranilate was found in the liver and kidney, while methyl 5-hydroxy-*N*-methylanthranilate was found in all analyzed organs except the spleen.

Generally, the hydroxylation of MMA and IMA is consistent with the metabolism of aromatic compounds that are being oxidized in the liver by cytochrome P450 enzymes to arenol metabolites (Williams, 2012; Radulović et al., 2017). This biotransformation occurs to increase the water solubility of the parent compounds for a possibly more efficient urinary excretion. We have already discussed the mechanism of MMA and IMA hydroxylation which possibly occurs via epoxide (arene oxide) intermediates, where electron-donating ($-NH_2$) groups direct the opening of the epoxide to form *ortho*- and *para*-hydroxy-derivatives with respect to that group (Radulović et al., 2017). The formation of isopropyl and methyl esters of 3-hydroxy-*N*-methylanthranilate is disfavored due to the steric hindrance imposed by the NHMe group; 3-HMMA was below the detection limits in the analyzed homogenates. The lower abundance of the hydroxylated metabolites in the analyzed organs in comparison to their content in the urine can be attributed to their faster excretion due to their higher hydrophilicity relative to the unmetabolized esters. Moreover, another possible scenario is that 1 h is simply not long enough for this metabolic pathway to yield significant amounts of the end products i.e. hydroxylated derivatives.

Previously, we found that the administration of MMA or IMA, on their own (200 mg kg^{-1}, *i.p.*, 7 days) did not cause changes in liver morphology and function (Radulović et al., 2013d, 2017). Considering the potential use of MMA and IMA as therapeutics, these findings are of great interest as the liver plays a central role in xenobiotic biotransformations and can be susceptible to possible toxic effects from xenobiotics or their metabolites (Radulović et al., 2017). Furthermore, the administration of both anthranilates exhibited a significant hepatoprotective potential in the model of acute intoxication with carbon tetrachloride (CCl_4) (Radulović et al., 2013d). Previously, we hypothesized that the antioxidant activity of MMA and IMA could not be the modus operandi behind this hepatoprotective effect since the compounds exerted no significant radical scavenging activity (Radulović et al., 2015). However, now, knowing that hydroxylated MMA and IMA metabolites are present in the livers, and considering their structure, *i.e.* electron-rich phenolics, one might suggest that the metabolites could play this antioxidant role and protect the organ from oxidative stress. This, naturally, requires additional experiments in order to be verified.

Moreover, phase II metabolites were found in the analyzed liver tissues; *N*-acetylanthranilic acid (AcAA), isopropyl *N*-acetylanthranilate (IAcA) and isopropyl 3-hydroxy-*N*-acetylanthranilate (3-HIAcA) in the liver of IMA-treated rats, and methyl *N*-formylanthranilate (MFA) and methyl 3(or 5)-hydroxy-*N*-acetylanthranilate (HMAcA) in the liver of MMA-treated rats. As we discussed in our previous study (Radulović et al., 2017), the principal detoxification pathway of arylamines is *N*-acetylation, catalyzed by arylamine *N*-acetyltransferases that utilize acetyl coenzyme A as a cofactor (Radulović et al., 2017 and literature cited therein).

The kidney-metabolite profile of IMA displayed only the unmetabolized IMA in quantifiable amounts, while other detected metabolites were present in traces. On the other hand, the hydrolysis product, NMAA, was present in the kidneys of rats treated with MMA in relatively high amounts (0.16 mg g^{-1} female rats and 0.08 mg g^{-1} male rats), followed by the unmetabolized MMA (0.10 mg g^{-1} female rats and 0.06 mg g^{-1} male rats). In one of our previous studies we found that both compounds administered on their own (200 mg kg^{-1}, *i.p.*, 7 days) did not influence kidney morphology and function and that only MMA, but not IMA, exhibited a nephroprotective activity in the CCl_4-induced kidney damage model in rats (Radulović et al., 2015). Having in mind the previously determined differences in the nephroprotective potentials of MMA and IMA (*i.e.* the lack of this potential for IMA) and their different kidney-metabolite profiles, we could speculate that the nephroprotective activity is due to the product of hydrolysis of anthranilate esters, *N*-methylanthranilic acid, that is the major anthranilate derivative found in the kidneys of MMA-, but not IMA-, treated animals. Although the nephroprotective effect is usually attributed to antioxidants, this does not appear to be the case for NMAA as it does not differ significantly in this radical capturing feature from MMA or IMA. It could be that also the phenolic derivatives contribute to this nephroprotective potential, hence, the possible protective activity of NMAA and these hydroxylated metabolites deserve further evaluation.

Furthermore, when compared to the content in other organs, the unmetabolized anthranilates were present in higher amounts in the brain tissue. For MMA the next most abundant compound in the brain was *N*-methylanthranilic acid, although it was not detected in the case IMA. In the amount greater than traces, *N*-demethylation product MA was found in the brain of male rats (0.01 mg g^{-1}), while IA was found in the brain of female rats (0.04 mg g^{-1}). Moreover, the brain tissue of MMA-treated rats contained AA, 5-HMMA, and MAn while for IMA, besides the parent anthranilate and IA, only BA was detected in traces.

In our previous study, both anthranilate esters exhibited effects on the central nervous system (CNS), including anxiolytic and antidepressant activities, and they both prolonged diazepam-induced sleep in mice (Radulović et al., 2013b). Generally, to exert psychoactive effects, a substance must enter the brain through the brain's chemical protection system, which consists mainly of the blood-brain barrier (BBB). BBB represents a major obstacle to the delivery of pharmacologically active substances to the CNS (SAMHSA and CSAT, 1999). The list of molecular properties associated with the distribution of a xenobiotic within an organism, especially those associated with BBB permeability, is given by Fong (2015), and Pajouhesh and Lenz (2005). These properties for all of the anthranilate metabolites detected in the organs of rats treated with MMA and IMA were calculated using Chem3D Ultra 16.0 (CambridgeSoft) and are given in Table 5.

Based on the calculated values, all anthranilates possess an adequate number of rotatable bonds, H-bond donor and acceptor atoms, as well as spherical molecular shape and molecular weight for unobstructed BBB passage (Fong, 2015; Pajouhesh and Lenz, 2005). For some of the anthranilates, cLogP, polar surface area, and pKa, to some extent, differ from the abovementioned criteria. For example, the parent compounds, MMA and IMA, have a cLogP value slightly higher (2.66 and 3.50, respectively) than it is set (1.5–2.5). Thus, small neutral molecules, such as MMA and IMA, and the unionized forms of their metabolites (NMAA, MA, 5-HMMA, MAn in the case of MMA and IA and BA in the case of IMA), detected in the brain tissue, would be expected to easily pass through the blood-brain barrier and enter the brain. AA was found in the brain tissue in the case of rats treated with MMA despite the low

Table 5
Molecular properties that influence the disposition of a compound within an organism, especially those associated with BBB permeability.

Compound	cLogP[a]	H-Bond Acceptors[a]	H-Bond Donors[a]	Mw	Polar Surface Area (Å^2)[a]	Ovality[a]	Rotatable Bonds[a]	pKa
	1.5–2.7[b]	< 7[b]	< 3[b]	< 400[b]	< 60–70[b]	< 5[b]	< 5[b]	4–10[b]
IMA	3.50	2	1	193.25	38.33	1.40	4	-[a]
IA	2.96	2	1	179.22	53.32	1.37	3	-[a]
3-HIMA	2.99	3	2	209.25	58.56	1.40	4	8.56[a]
3-HIA	2.48	3	2	195.22	72.55	1.38	3	8.47[a]
5-HIMA	2.99	3	2	209.25	58.56	1.41	4	8.78[a]
5-HIA	2.48	3	2	195.22	72.55	1.39	3	8.84
MMA	2.66	2	1	165.19	38.33	1.32	3	-[a]
MA	2.12	2	1	151.16	52.32	1.32	2	-[a]
								2.23 (ammonium salt, Perrin, 1965)
3-HMMA	2.16	3	2	181.19	58.56	1.31	3	8.59[a]
3-HMA	1.64	3	2	167.16	72.55	1.32	2	8.51[a]
5-HMMA	2.16	3	2	181.19	58.56	1.34	3	8.82[a]
5-HMA	1.64	3	2	167.16	72.55	1.33	2	8.88[a]
NMAA	2.36	2	2	151.16	49.33	1.29	2	3.86[a]
AA	1.21	2	2	137.14	63.32	1.26	1	3.90[a]
								2.14 (Kortum et al., 1961)
An	0.92	1	1	93.13	26.02	1.22	0	-[a]
								4.60 (ammonium salt, Perrin, 1972)
MAn	1.64	1	1	107.16	12.03	1.27	1	-[a]
								4.85 (ammonium salt, Riddick et al., 1985)
BA	1.88	1	1	122.12	37.30	1.25	1	4.25[a]
								4.20 (Haynes, 2010)
MFA	1.68	2	1	179.18	55.40	1.33	4	-[a]
3-HMAcA	1.37	3	2	209.20	75.63	1.32	4	6.71[a]
5-HMAcA	1.14	3	2	209.20	75.63	1.40	4	8.27[a]
AcAA	1.83	2	2	179.18	66.40	1.34	3	3.54[a]
IAcA	2.44	2	1	221.26	55.40	1.44	5	0[a]
3-HIAcA	2.21	3	2	237.26	75.63	1.42	5	6.67[a]
3-HIB	2.82	2	1	180.20	46.52	1.37	3	8.47[a]

[a] Calculated using Chem3D Ultra 16.0.
[b] Value required to meet the criteria given by Fong (2015), and Pajouhesh and Lenz (2005).

cLogP value and lower limit pKa value. As the other parameters meet the criteria, AA was probably able to pass BBB. Another possibility is that some of the metabolites (in particular products of MMA and IMA hydrolysis and/or *N*-demethylation) are formed in the brain from the parent compounds, as these biotransformation pathways, can also occur in extrahepatic organs, including the brain.

For MMA, GC-MS analysis of the quadriceps femoris muscle homogenate extracts revealed the presence of the unmetabolized anthranilate (tr – female rats, 0.06 mg g^{-1} – male rats) and NMAA (0.06 mg g^{-1} – female rats, tr – male rats), as well as traces of MA and 5-HMMA in the mentioned tissue of rats of both gender. On the other hand, in the case of IMA, neither the parent compound nor the corresponding metabolites were detected in the skeletal muscles. In our previous studies, we ruled out the possible effects of IMA and MMA on the locomotor performance (Gomes Pinheiro, 2014; Radulović et al., 2013) in the open-field, horizontal-wire, and rotarod tests. The open-field test demonstrated that anthranilates do not influence the general locomotion in a novel arena, while horizontal-wire and rotarod tests showed that tested compounds are not a general motor stimulant and that they do not exhibit muscle relaxant effects. Generally, there are two possible modes of action of muscle relaxant substances: neuromuscular blockers act peripherally as skeletal muscle relaxants, which block neuromuscular junction function and they have no CNS activity; centrally acting skeletal muscle relaxants are commonly indicated to alleviate two different conditions: spasticity and muscular pain or spasms (Vardanyan and Hruby, 2016).

Cardiac tissue of MMA-treated rats contained high amounts of NMAA (ca. 0.3 mg g^{-1}, rats of both gender), followed by the unmetabolized MMA (0.04 and 0.02 mg g^{-1}, female and male rats, respectively) and AA (0.04 mg g^{-1} and tr, female and male rats, respectively), while MA, 5-HMMA and MAn were present in traces. Heart tissue of the male rats treated with IMA contained 0.07 mg of the unmetabolized IMA per gram of the tissue, while in the case of female rats it was present only in traces. Trace amounts of NMAA, IA, MAn, BA, AcAA, and IAcAA were present in the heart of IMA-treated rats. The lungs of female rats treated with MMA contained 0.02 mg of MMA and NMAA per gram of the analyzed tissue, while in the case of male rats the parent compound was present in traces and NMMA was present in the amount approximately the same as in the case of female rats. AA, 5-HMMA, and MAn were present in traces. Lungs of female rats treated with IMA contained ca. 0.05 mg g^{-1} of IMA and NMAA but these two compounds were present in traces in the lungs of male rats. Other detected metabolites were: IA, AA, MAn, BA, 3-HIB, IAcA. In the case of MMA, the unmetabolized compound was present at 0.05 mg g^{-1} in the spleen of male rats, though in female rats it was present only in traces, while in the case of IMA, the spleen of rats of both genders contained trace amounts of unmetabolized IMA. Also, the spleen of rats administered with MMA/IMA contained NMAA and MA/IA in traces (Tables 1 and 2).

We wished to determine whether the dose of the administered compound influences the organ-metabolite profile. This is why we repeated our experiments with a significantly higher dose, 5 g kg^{-1}, of MMA and IMA administered to the animals. Although the chemical composition of the extracts of organ homogenates was qualitatively the same as in the case of the dose of 2 g kg^{-1}, there were several differences in the relative abundances of some metabolites. For IMA, the major difference was that the dose of 5 g kg^{-1} resulted in the detection of a high amount of the unmetabolized compound in the spleen tissue (3.8 mg g^{-1}) in comparison to its content in other organs (liver, kidneys, heart, and lungs tissues contained 0.5, 0.5, 0.2 and 0.4 mg of IMA per gram of the tissue sample, respectively), whereas at the dose of 2 g kg^{-1} the spleen contained only traces of unmetabolized IMA. Another peculiarity is that the relative ratio of NMAA and IMA in the liver and kidneys of IMA-treated rats, at the dose 5 g kg^{-1}, was

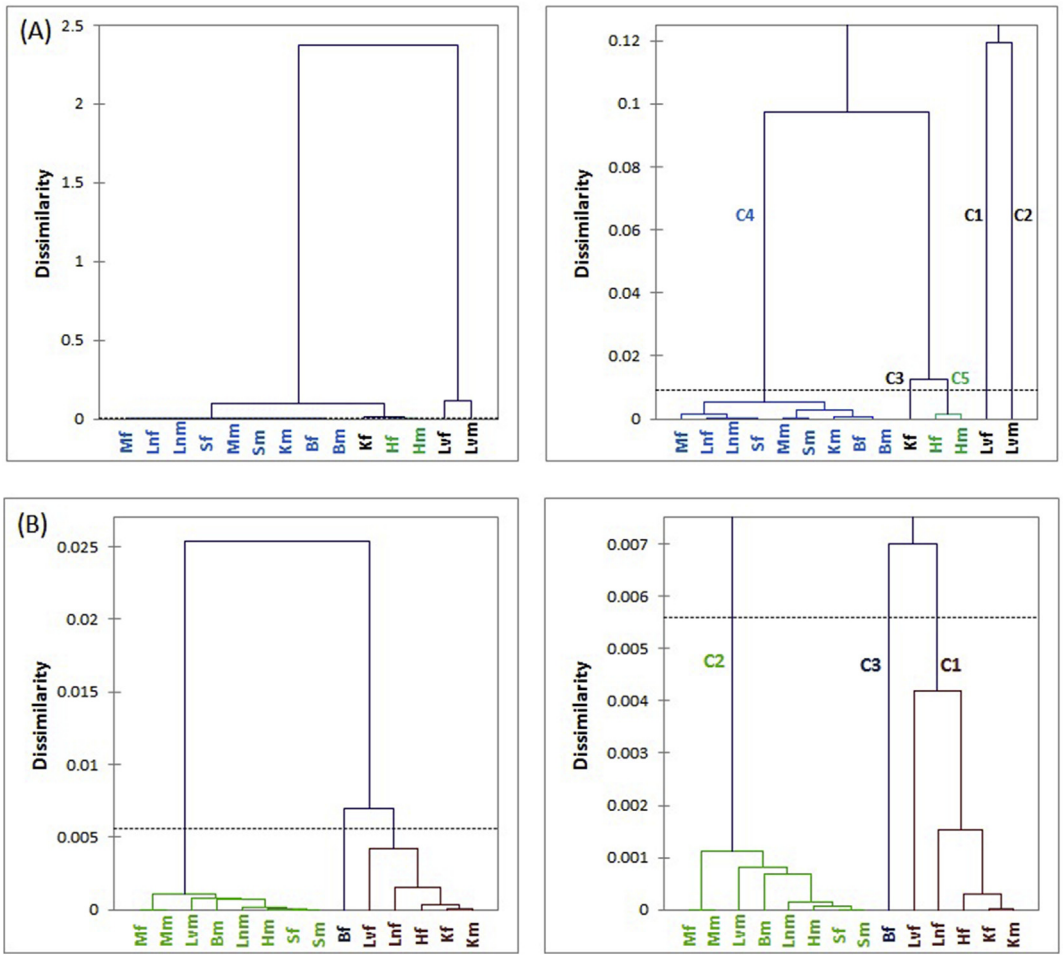

Fig. 2. Dendrograms (left) and the corresponding expansions (right) (AHC analysis) representing the chemical-composition dissimilarity relationships of metabolite organ profiles of rats treated with MMA (A) and IMA (B) (observations) obtained by agglomerative hierarchical clustering using Euclidian distances as dissimilarity metric and the masses of the parent compound or corresponding anthranilate-related metabolites in milligrams per gram of the organ as variables. Dissimilarity was within the intervals [0–2.5], and [0–0.025], respectively, and Ward's method was used as the aggregation criterion. (Lvf – liver (female), Lvm – liver (male), Kf – kidneys (female), Km – kidneys (male), Hf – heart (female), Hm – heart (male), Bf – brain (female), Bm – brain (male), Lnf – lungs (female), Lnm – lungs (male), Mf – quadriceps femoris muscles (female), Mm – quadriceps femoris muscles (male), Sf – spleen (female), Sm – spleen (male)).

significantly higher than at 2 g kg^{-1}. At 5 g kg^{-1}, the liver contained 0.8 mg g^{-1} of NMAA and 0.5 mg g^{-1} IMA, while the kidneys contained ca. 0.5 mg g^{-1} of both compounds (cf. the values of NMAA and IMA for the dose of 2 g kg^{-1} in Table 4). In the case of MMA, the major difference was that the 2.5-times higher dose of MMA resulted in ca. 10 times higher amount of MMA (0.5 mg g^{-1}) and NMAA (0.7 mg g^{-1}) in the brain tissue (at the dose 2 g kg^{-1}, a gram of the brain tissue contained 0.06 mg of MMA and 0.04 mg of NMAA).

Based on the qualitative similarity of organ-metabolite profiles of MMA and IMA, one may conclude that they both undergo the same biotransformation pathways. However, the principal difference lays in the relative abundance of the analogous metabolites. Comparing the summed amount of a specific metabolite (recalculated to the mass of the administered compound) in the analyzed tissues in the case of MMA, the principal MMA metabolites were the products of ester hydrolysis, NMAA (1.57 and 1.25 mg per gram of all analyzed organs of female and male rats, respectively) and AA (1.46 and 0.85 mg g^{-1} for female and male rats, respectively), while the unmetabolized MMA was present in relatively low amounts (0.26 mg g^{-1}, rats of both gender), followed by MA (tr and 0.01 female and male rats, respectively). On the other hand, for rats treated with IMA, the unmetabolized compound was the most abundant (0.48 and 0.11 mg g^{-1}) anthranilate-related compound in the organs of female and male rats, respectively, followed by NMAA (0.16 and 0.03 mg g^{-1}) and IA (0.04 mg g^{-1} and tr).

Organ-metabolite profile of female and male rats treated with MMA and IMA were qualitatively similar. However, there were evident gender-related differences in the quantitative distribution of particular metabolites. For MMA-treated rats, it seemed that male rat organs contained the same or approximately ½ times lower quantity of certain metabolites, with the exception of the spleen and skeletal muscles. Alternatively, in the case of rats treated with IMA, this difference was even more pronounced and the organs of female and male rats were clearly separated in the dendrogram obtained as the result of AHC analyses (as detailed in subsection 3.1.).

3.1. Multivariate statistical analysis (MVA)

In order to better describe the organ-metabolite profiles, we statistically compared the compositional (quantitative) data from the GC-MS analysis of the diethyl-ether extracts of the selected tissues of rats treated with MMA or IMA (Tables 3 and 4) by performing multivariate statistical analysis (MVA). Agglomerative hierarchical clustering (AHC) and principal component analysis (PCA), that facilitated the interpretation of the data and allowed us to make statistically supported conclusions, were performed using the Excel program plug-in XLSTAT. Both methods were applied utilizing the content of the extract constituents in mg per gram of the analyzed tissue as original variables (only constituents that were present in the organs in the amounts higher

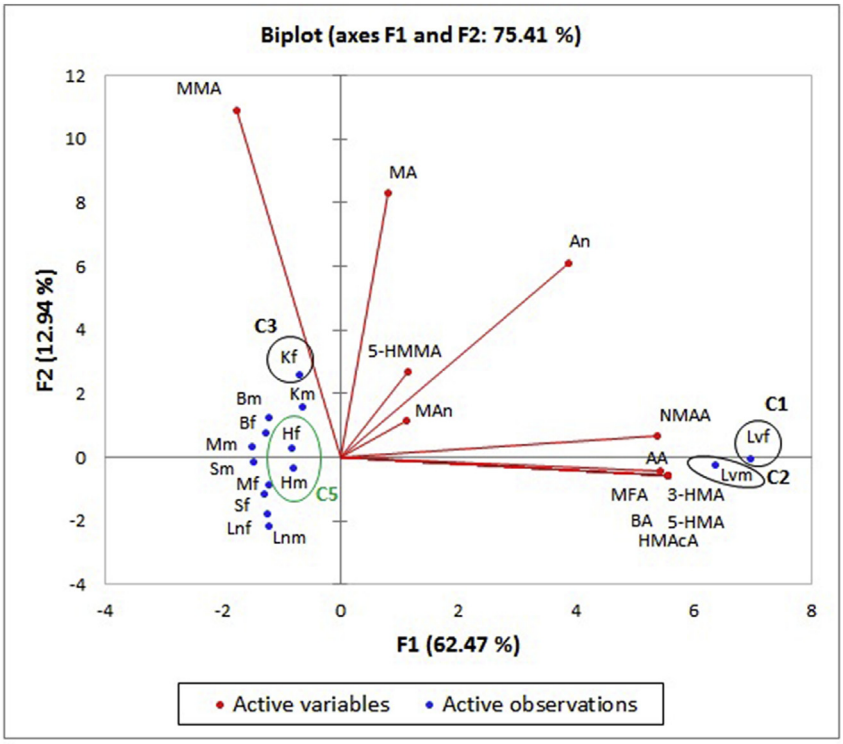

Fig. 3. The plot of the ordination of organ-metabolite profiles and of the variables, obtained by principal component analysis (PCA; mg of anthranilate-related compounds per gram of the organ used as variables) related to the organs of rats treated with MMA. Axes (F1 and F2 factors, the first and second principal components, respectively) refer to the ordering scores obtained from the samples. Axis F1 accounts for ca. 62% and axis F2 for a further 13% of the total variance. (Lvf – liver (female), Lvm – liver (male), Kf – kidneys (female), Km – kidneys (male), Hf – heart (female), Hm – heart (male), Bf – brain (female), Bm – brain (male), Lnf – lungs (female), Lnm – lungs (male), Mf – quadriceps femoris muscles (female), Mm – quadriceps femoris muscles (male), Sf – spleen (female), Sm – spleen (male)).

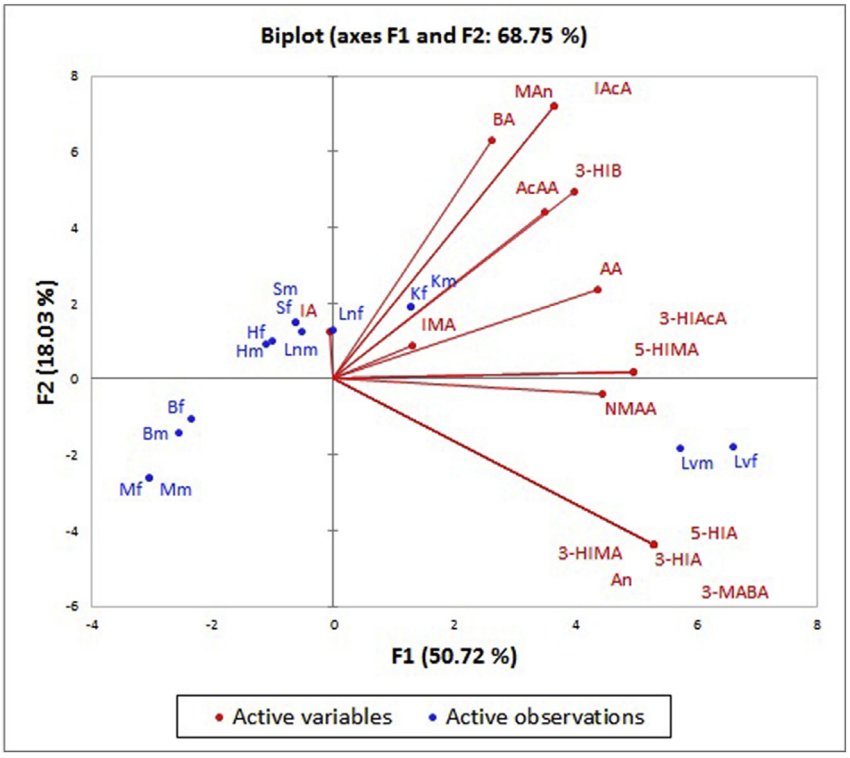

Fig. 4. The plot of the ordination of organ-metabolite profiles and of the variables, obtained by principal component analysis (PCA; mg of anthranilate-related compounds per gram of the organ used as variables) related to the organs of rats treated with IMA. Axes (F1 and F2 factors, the first and second principal components, respectively) refer to the ordering scores obtained from the samples. Axis F1 accounts for ca. 51% and axis F2 for a further 18% of the total variance. (Lvf – liver (female), Lvm – liver (male), Kf – kidneys (female), Km – kidneys (male), Hf – heart (female), Hm – heart (male), Bf – brain (female), Bm – brain (male), Lnf – lungs (female), Lnm – lungs (male), Mf – quadriceps femoris muscles (female), Mm – quadriceps femoris muscles (male), Sf – spleen (female), Sm – spleen (male)).

than 0.009 and 0.01 mg g^{-1} in the case of rats treated with MMA and IMA, respectively, were taken into account). The results of AHC and PCA are illustrated in Fig. 2 – 4.

Based on AHC analysis, the organs of rats treated with MMA were grouped into five statistically different classes, C1–C5 (Fig. 2A). Three classes, C1, C2, and C3, were composed of only a single organ. Classes C1 and C2, i.e. the metabolite profiles of the livers of female and male rats, respectively, were clearly separated from the others within a pure clade, with AA and NMAA as the most abundant anthranilates quantified. High amounts of the unmetabolized MMA, together with NMAA, made the profile of female kidney tissue sufficiently distinct from the other organ profiles to form a separate class C3 that belonged to the second clade visible on the dendrogram. The metabolite profiles of the heart tissues of female and male rats comprised C5, a sister group in the same subclade with C3, characterized by a significant content of NMAA and approximately 10 times lower amount of MMA. Class C4 was quite

heterogeneous, circumscribing all other analyzed organs. Grouping of the samples in the PCA plot (Fig. 3) was in general accordance with the results of the corresponding AHC analyses. The PCA analysis has revealed strong dependencies between some metabolites (expressed as correlation coefficients, r). High coefficients ($r > 0.9$) were noted among NMAA, AA, 3-HMA, 5-HMA, BA, HMAcA, and MFA. Also, the dependencies between hydroxylated MMA metabolites, 3-HMA, 5-HMA, and HMAcA, were revealed with mutual maximum correlation coefficients ($r = 1$), and this is not surprising as they are part of the same biosynthetic pathway. On the other hand, 5-HMMA did not show a strong correlation with other hydroxylated metabolites (r between 5-HMMA and 3-HMA, 5-HMA, and HMAcA was only 0.167). This could be possibly mean that hydroxylation of the *N*-methylated molecules occurs independently from the *N*-demethylated ones.

The dendrogram obtained as the result of AHC analysis of IMA organ profiles is depicted in Fig. 2B and it delimitates three statistically different classes of organs (C1-C3). One of the clades was almost exclusively composed of organs of female rats (brain, liver, kidneys, heart, and lungs) with an exception of the kidneys of male rats. Except for the brain tissue, all of the samples belonged to the same class C1. For all of them, the most abundant constituent was the unmetabolized IMA. All organs of male rats, with the exception of the mentioned kidneys, as well as spleen and muscle tissues of female rats, comprised the most populated clade that was only a single class C2. Organs from this class (C2) were segregated in two subclades, according to the identity and relative abundances of their constituents. Unsurprisingly, the muscle tissues of rats of both genders formed a single subclade within C2 as they contained neither the parent compound nor the corresponding metabolites. Livers of the male rats comprised another subsubclade within C2, characterized by the presence of all detected metabolites (albeit) in traces and NMAA in the amount of 0.02 mg g^{-1}. The third C2 subclade was the most populated one comprising the heart, brain, and lungs of male rats and the spleens of the rats of both genders. The mentioned profile of the brain tissue of female rats displayed the highest amount of the unmetabolized IMA (0.16 mg g^{-1}), followed by the highest content of IA (0.04 mg g^{-1}), and BA in traces, forming on its own a separate class - C3 (Fig. 2B). An interesting feature is that the brain was the only organ where no NMAA and AA were found (except the skeletal muscles where neither of the anthranilate-related compounds was detected).

According to the results of PCA (biplot is given in Fig. 4), the matching organs of female and male rats were highly similar based on the abundance of their components. Due to the relatively high content of NMAA, the livers of female and male rats were grouped together, while the high content of the unmetabolized IMA placed the kidneys of rats of both genders near each other. Also, the brains of rats of both gender, as well as the skeletal muscles were grouped together, being in agreement with AHC results. In the case of IMA treated rats, PCA did not reveal strong dependences between metabolites except between the hydroxylated ones. Again, for 3-HIA, 3-HIMA, and 5-HIA, the correlation coefficients (r) were 1.0. Conversely, as in the case of MMA metabolites, the content of 5-HIMA did not strongly correlate with the aforementioned hydroxylated metabolites (this time the value of r was higher, 0.645). It seems that MVA is a useful exploratory tool probing the biotransformation pathways of xenobiotics: a quantitative, mathematical relationship following the general linear form between individual compounds in organ-metabolite profile would suggest that the biotransformation of such chemicals is not only closely related but may involve either the same enzyme system or at least a common intermediate.

4. Conclusions

To summarize, in this paper, the metabolism of two polypharmacologically active *Choisya ternata* essential-oil constituents, methyl (MMA) and isopropyl *N*-methylanthranilates (IMA), were investigated. GC-MS analysis of the diethyl-ether extracts of selected tissues of rats treated with MMA and IMA enabled the identification of 12 and 16 anthranilate-related compounds, respectively. Organ-metabolite profiles of MMA and IMA were qualitatively mutually analogous (varying only in the alcohol moiety of the metabolites), and generally analogous to the previously investigated urinary-metabolite profiles (Radulović et al., 2017). The greatest diversity and the highest overall amount of anthranilate metabolites was found in the hepatic tissue, that is not surprising as the liver plays the main role in the detoxification process. The principal anthranilate-related compounds in the organs of rats treated with MMA were the products of ester hydrolysis *N*-methylanthranilic acid and anthranilic acid, followed by the unmetabolized MMA and methyl anthranilate, while other metabolites were present in traces. For rats treated with IMA, the unmetabolized compound was the most abundant in organs of both female and male rats, followed by *N*-methylanthranilic acid and isopropyl anthranilate. Hydroxylated metabolites, that were the major metabolites found in the urine of rats treated with IMA, were detected in organs only in traces, while 2-(methylamino)benzamide, the principal metabolite found in the urine of MMA-treated rats, was not detected at all or was a very minor xenobiotic metabolite. A collection of the compositional data regarding the anthranilate-related metabolites was statistically treated by MVA that provided a better insight into the possible biotransformation pathways. These results, that are a starting point for further ADMET and related studies, are of importance considering the constant oral and cutaneous human exposure to MMA, as well as the potential therapeutic uses of both analyzed anthranilate esters having in mind their polypharmacological, panacea-like properties (antinociceptive, anti-inflammatory, gastro-, hepato- and nephroprotective activities, anxiolytic and antidepressant properties, as well as an effect on diazepam-induced sleep).

Acknowledgment

This work was supported by the Ministry of Education, Science and Technological Development of the Republic of Serbia [Project No. 172061].

Transparency document

Transparency document related to this article can be found online at https://doi.org/10.1016/j.fct.2019.03.039.

References

Bakkali, F., Averbeck, S., Averbeck, D., Idaomar, M., 2008. Biological effects of essential oils – a review. Food Chem. Toxicol. 46, 446–475.

EU Directive 2010/63/EU For Animal Experiments. Legislation for the Protection of Animals Used for Scientific Purposes. http://ec.europa.eu/environment/chemicals/lab_animals/legislation_en.htm, Accessed date: 15 January 2019.

Fong, C.W., 2015. Permeability of the blood-brain barrier: molecular mechanism of transport of drugs and physiologically important compounds. J. Membr. Biol. 248, 651–669.

Fura, A., 2006. Role of pharmacologically active metabolites in drug discovery and development. Drug Discov. Today 11, 133–142.

Gaunt, I.F., Sharratt, M., Grasso, P., Wright, M., 1970. Acute and short-term toxicity of methyl-*N*-methyl anthranilate in rats. Food Cosmet. Toxicol. 8, 359–368.

Gomes Pinheiro, M.M., Miltojević, A.B., Radulović, N.S., Abdul-Wahab, I.R., Boylan, F., Fernandes, P.D., 2015. Anti-inflammatory activity of *Choisya ternata* Kunth essential oil, ternanthranin, and its two synthetic analogs (methyl and propyl *N*-methylanthranilates). PLoS One 10, e0121063.

Gomes Pinheiro, M.M., Radulović, N.S., Miltojević, A.B., Boylan, F., Fernandes, P.D., 2014. Antinociceptive esters of *N*-methylanthranilic acid: mechanism of action in heat-mediated pain. Eur. J. Pharmacol. 727, 106–114.

Haynes, W.M. (Ed.), 2010. CRC Handbook of Chemistry and Physics, ninety-first ed. CRC Press Inc., Boca Raton, FL, pp. 8–47.

Heymann, E., 1980. Carboxylesterases and amidases. In: Jakoby, W.B. (Ed.), Enzymatic Basis of Detoxication, Vol II, second ed. Academic Press, New York, pp. 291–323.

Kortum, G., Vogel, W., Andrussow, K., 1961. International Union of Pure and Applied Chemistry. Commission on Electrochemical Data. Dissociation Constants of Organic Acids in Aqueous Solution. International Union of Pure and Applied Chemistry. London, Butterworth.

Macherey, A.-C., Dansette, P.M., 2008. Biotransformations leading to toxic metabolites: chemical aspect. In: Wermuth, C.G. (Ed.), The Practice of Medicinal Chemistry. Academic Press, Burlington, MA, pp. 674–696.
Miltojević, A.B., Radulović, N.S., Stojanović, N.M., Randjelović, P.J., 2018. Polypharmacologically active esters of *N*-methylanthranilic acid from Mexican orange (*Choisya ternata* Kunth): from the discovery to panacea-like properties. In: Proceedings of the 8th Conference of Serbian Biochemical Society, pp. 53–65.
Mitra, A.K., Kwatra, D., Vadlapudi, A.D., 2014. Drug Delivery, first ed. Jones & Bartlett Publishers, Burlington, MA.
Naito, J., Sasaki, E., Ohta, Y., Shinohara, R., Ishiguro, I., 1984. Anthranilic acid metabolism in the isolated perfused rat liver: detection and determination of anthranilic acid and its related substances using high-performance liquid chromatography with electrochemical detection. Biochem. Pharmacol. 33 3195e3200.
Pajouhesh, H., Lenz, G.R., 2005. Medicinal chemical properties of successful central nervous system drugs. NeuroRx 2, 541–553.
Perrin, D.D., 1965. Dissociation Constants of Organic Bases in Aqueous Solution. IUPAC Chemical Data Series, Buttersworth, London.
Perrin, D.D., 1972. Dissociation Constants of Organic Bases in Aqueous Solution. IUPAC Chemical Data Series: Supplements. Buttersworth, London.
Radulović, N.S., Jovanović, I., Ilić, I.R., Randjelović, P.J., Stojanović, N.M., Miltojević, A.B., 2013a. Methyl and isopropyl *N*-methylanthranilates attenuate diclofenac- and ethanol-induced gastric lesions in rats. Life Sci. 93, 840–846.
Radulović, N.S., Miltojević, A.B., McDermott, M., Waldren, S., Parnell, J.A., Pinheiro, M.M.G., Fernandes, P.D., Menezes, F.d.S., 2011. Identification of a new antinociceptive alkaloid isopropyl *N*-methylanthranilate from the essential oil of *Choisya ternata* Kunth. J. Ethnopharmacol. 135, 610–619.
Radulović, N.S., Miltojević, A.B., Randjelović, P.J., Stojanović, N.M., Boylan, F., 2013b. Effects of methyl and isopropyl *N*-methylanthranilates from *Choisya ternata* Kunth (Rutaceae) on experimental anxiety and depression in mice. Phytother Res. 27, 1334–1338.
Radulović, N.S., Miltojević, A.B., Stojanović, N.M.,, Randjelović, P.J., 2017. Distinct urinary metabolite profiles of two pharmacologically active *N*-methylanthranilates: three approaches to xenobiotic metabolite identification. Food Chem. Toxicol. 109, 341–355.
Radulović, N.S., Mladenović, M.Z., Blagojević, P.D., Stojanović-Radić, Z.Z., Ilić-Tomić, T., Senerović, L.B., Nikodinović-Runić, J., 2013c. Toxic essential oils. Part III: identification and biological activity of new allylmethoxyphenyl esters from a Chamomile species (*Anthemis segetalis* Ten.). Food Chem. Toxicol. 62, 554–565.
Radulović, N.S., Randjelović, P.J., Stojanović, N.M., Ilić, I.R., Miltojević, A.B., 2013d. Influence of methyl and isopropyl *N*-methylantranilates on carbon tetrachloride-induced changes in rat liver morphology and function. F.U. Phy. Chem. Technol. 11, 67–73.
Radulović, N.S., Randjelović, P.J., Stojanović, N.M., Ilić, I.R., Miltojević, A.B., Stojković, M.B., Ilić, M., 2015. Effect of two esters of *N*-methylanthranilic acid from Rutaceae species on impaired kidney morphology and function in rats caused by CCl_4. Life Sci. 135, 110–117.
Riddick, J.A., Bunger, W.B., Sakano, T.K., 1985. Organic Solvents: Physical Properties and Methods of Purification (Techniques of Chemistry), fourth ed. John Wiley and Sons, New York.
SAMHSA and CSAT, 1999. Substance abuse and mental health services administration and center for substance abuse treatment (US), 1999. How stimulants affect the brain and behavior. In: Treatment for Stimulant Use Disorders, Treatment Improvement Protocol (TIP) Series, No. 33.
SCCS (Scientific Committee on Consumer Safety), 2011. Opinion on Methyl *N*-Methylanthranilate. (Phototoxicity only). https://ec.europa.eu/health/scientific_committees/consumer_safety/docs/sccs_o_075.pdf, Accessed date: 15 January 2019.
Tisserand, R., Young, R., 2014. Essential Oil Safety: A Guide for Health Care Professionals, second ed. Churchill Livingstone, London.
Ufer, M., Juif, P.E., Boof, M.L., Muehlan, C., Dingemanse, J., 2017. Metabolite profiling in early clinical drug development: current status and future prospects. Expert Opin. Drug Metabol. Toxicol. 13, 803–806.
Van Den Dool, H., Kratz, P.D., 1963. A generalization of the retention index system including linear temperature programmed gas-liquid partition chromatography. J. Chromatogr. 11, 463–471.
Vardanyan, R., Hruby, V., 2016. Centrally acting skeletal muscle relaxants. In: Vardanyan, R., Hruby, V. (Eds.), Synthesis of Best-Seller Drugs. Academic Press, pp. 243–246.
Williams, D.A., 2012. Drug metabolism. In: Lemke, T.L., Williams, D.A., Roche, W.F., Zito, S.W. (Eds.), Foye's Principles of Medicinal Chemistry, seventh ed. Lippincott Williams & Wilkins, Philadelphia, pp. 106–190.
Yamaori, S., Yokozuka, H., Sasama, A., Funahashi, T., Kimura, T., Yamamoto, I., Watanabe, K., 2005. Hepatic metabolism of methyl anthranilate and methyl *N*-methylanthranilate as food flavoring agents in relation to allergenicity in the Guinea pig. J. Health Sci. 51, 667–675.